Optimization studies of the LPP short-wave radiation source with Xe gas jet target in the Ioffe Institute

S. G. Kalmykov, M. E. Sasin, R. P. Seisyan

A. F. Ioffe Physico-Technical Institute, St. Petersburg, Russia
serguei.kalmykov@mail.ioffe.ru

Introduction

- For several recent years, we were involved, in the Ioffe, into development and construction of a small, laboratory-type photolithographer using the EUV-range radiation.
- Not being restricted with high productivity demand, we could afford to choose the LPP source with Xe gas jet target due to its technical simplicity.
- Tentative experiments with the Xe gas jet target LPP source in the Ioffe 2003-2005 had demonstrated η_{conv} = 0.05-0.1%.
- The best world practice – 0.6-0.8%.
- Theoretical limit for the equilibrium plasma – 1.5%.

Therefore we ought to start our activity from optimization studies.

Our main idea

is combination of the KrF excimer laser for the fastest possible primary ionization with the Nd:YAG laser for subsequent plasma maintenance.

Effective multiphoton ionization of Xe by the UV λ = 248 nm laser gives a hope to complete the 1st ionization stage for a few very beginning nanoseconds.

When resuming our activity in 2009, before to commence on plasma experiments with the supersonic microjet targets, we had decided to carry out two preliminary works.

Results of both of them are to be presented at the evening poster session (P12 and P13).

A study of the laser produced plasma in stationary gases at low pressures (Poster session, P13)

- Nd:YAG laser, λ = 1,06 μm, E_{las} up to 1.4 J, typical energy introduced into the plasma – 0.5-0.6 J.
- Gases used: H_2, He, Ar, Xe.
- Pressure range – 1 Torr to 1 atm – corresponded to gas densities expected in the target jet – 10^{17} to 10^{18} cm^{-3}.

Laser plasma photographs taken with long expositions

Air

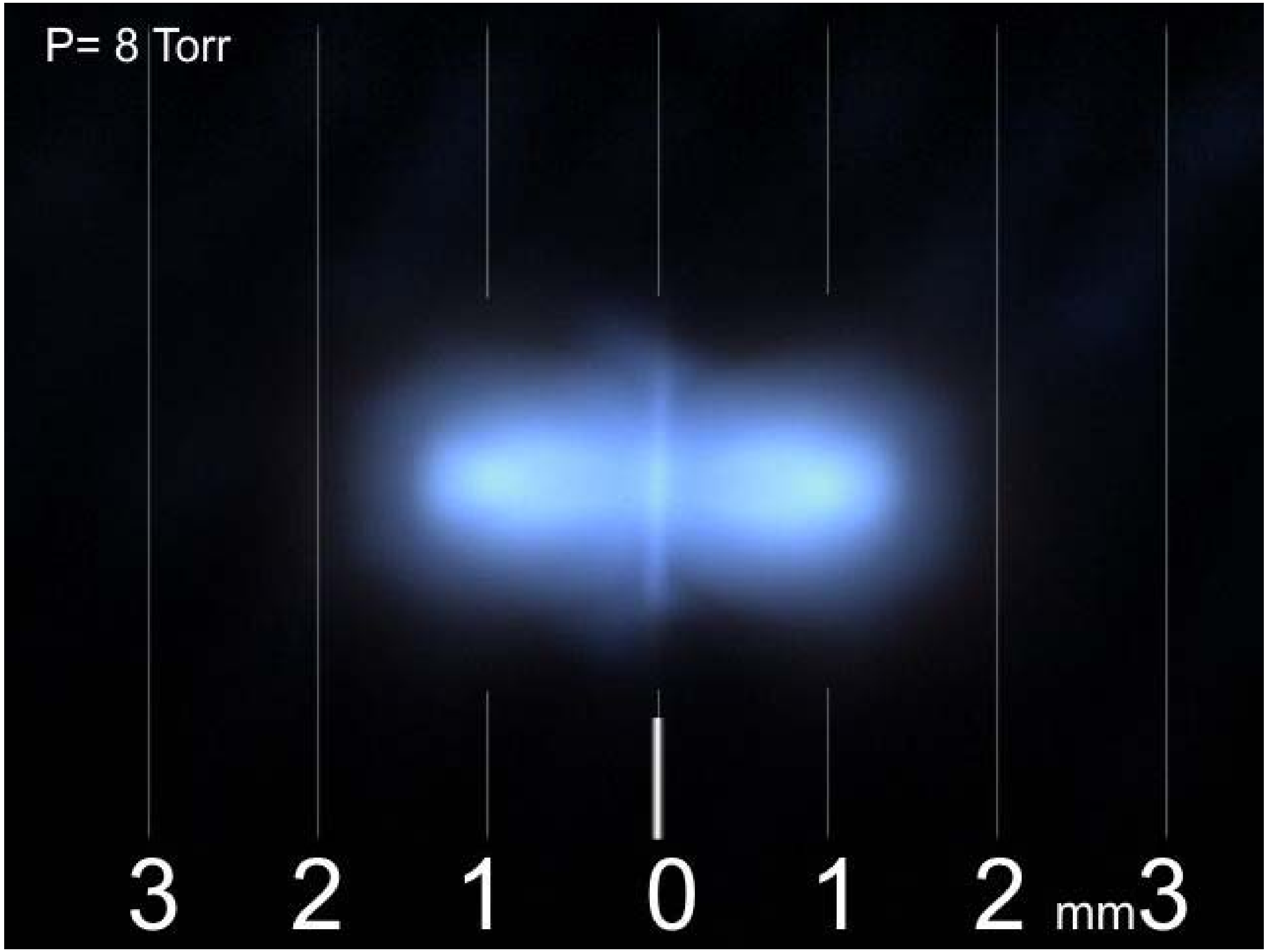

H_2

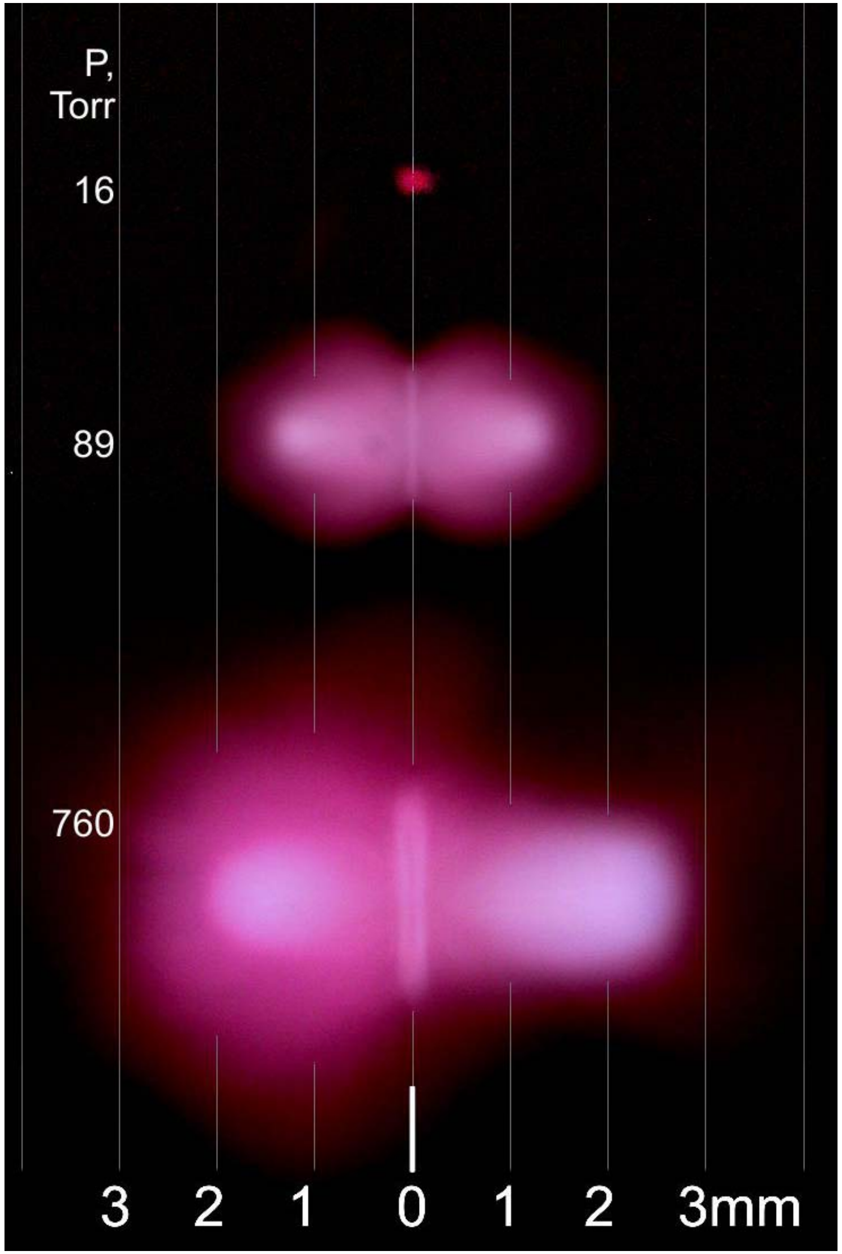

He

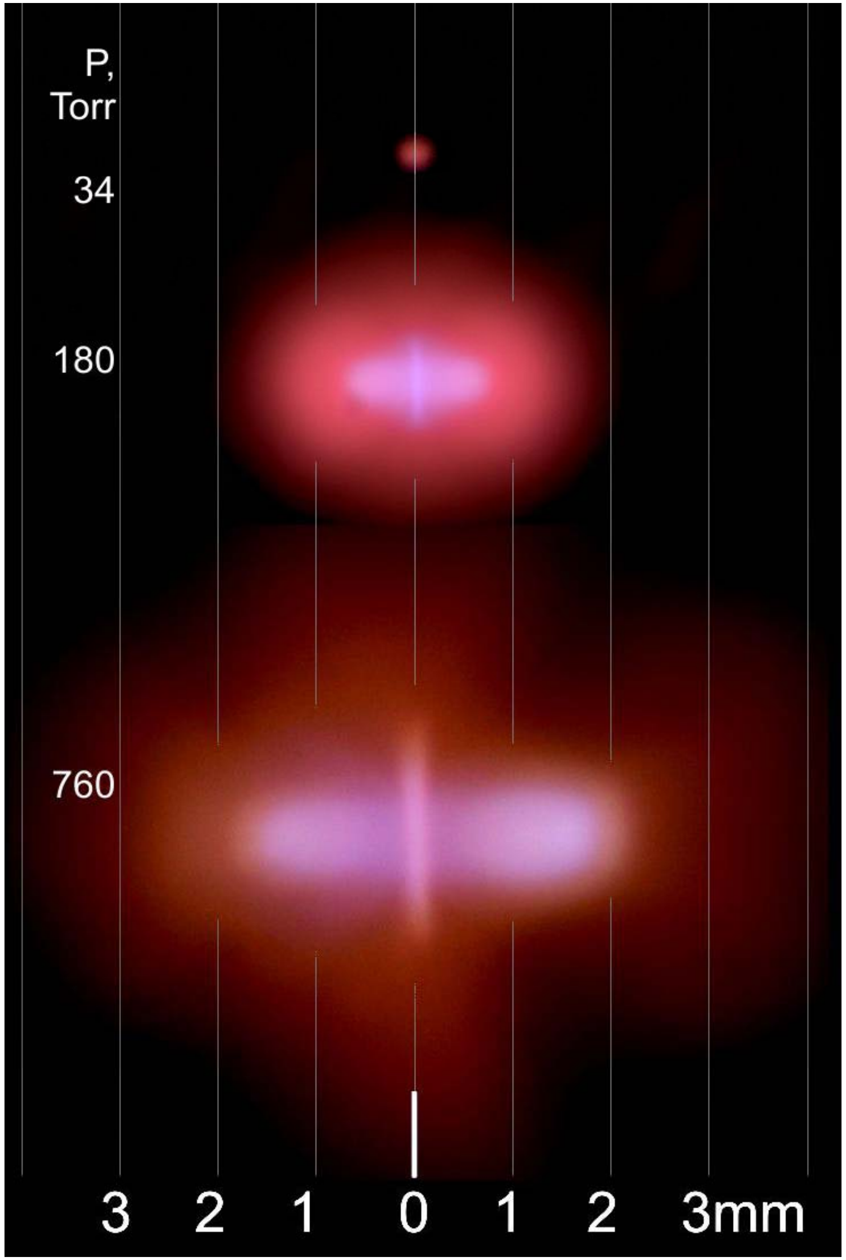

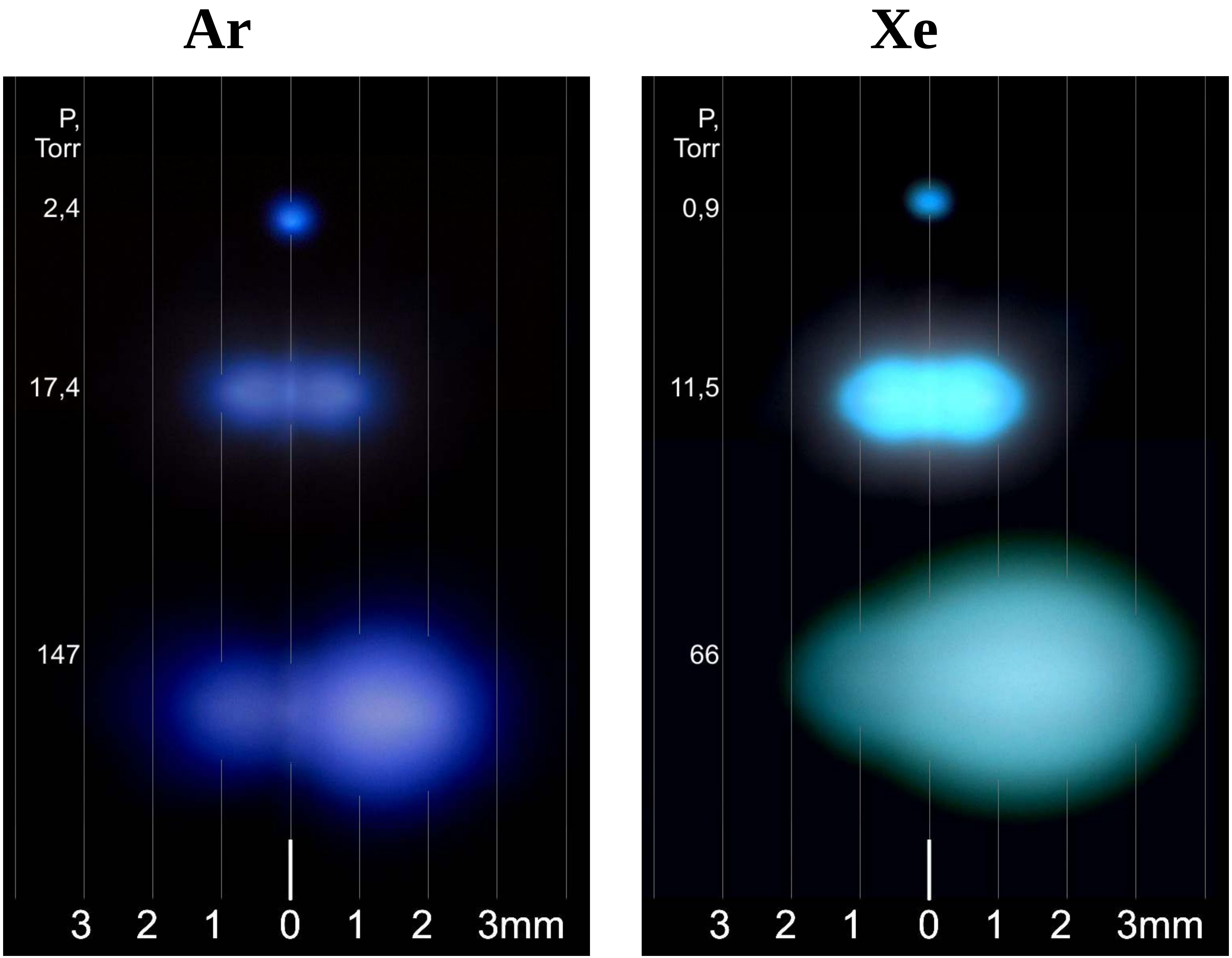
Ar
Xe
P,
Torr
2,4
17,4
147
3 2 1 0 1 2 3mm
P,
Torr
0,9
11,5
66
3 2 1 0 1 2 3mm

Ar, P = 23 Torr (n = 8.3×10^{17} cm^{-3}),
E_{las} = 0.63 J, I_{abs}/I_0 = 2%

Xe, P = 11.5 Torr (n = 4.1×10^{17} cm^{-3}),
E_{las} = 0.60 J, I_{abs}/I_0 = 1.7%.

Xe, P = 96 Torr (n = 3.4×10^{18} cm^{-3}),
E_{las} = 0.60 J, I_{abs}/I_0 = 93%.

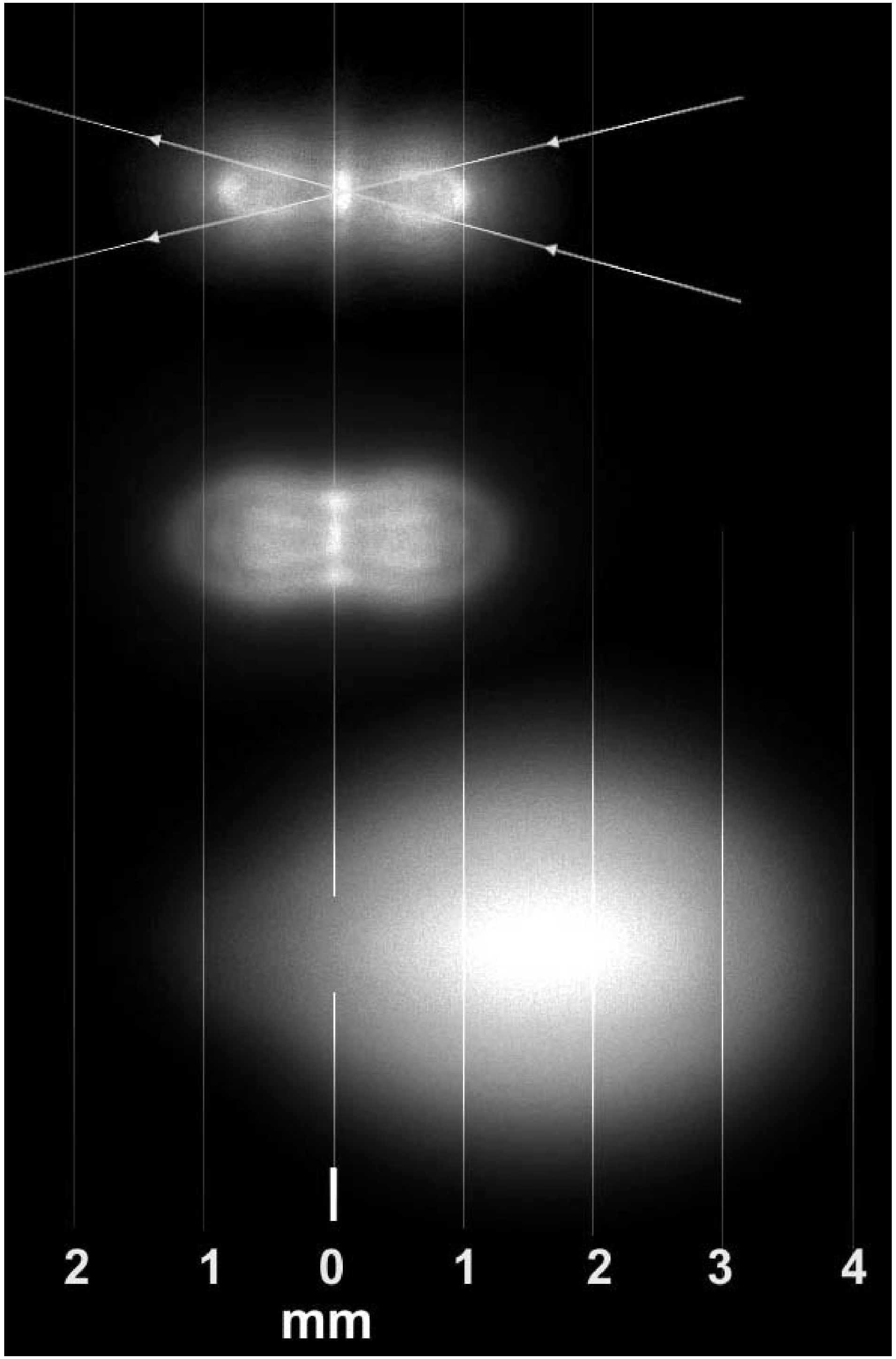

Long exposition spark photographs reveal some specific features of the low pressure laser plasmas:

- at the lowest pressures, the plasma emerges in the near-focus area as a sphere of 100-150 μm radius;
- plasma body has a symmetric, elongated form which follows, in general, to the form of the laser beam converging to the focus and diverging after;
- very complicated spatial spark structure is clearly seen, by now we have no explanations for most of the features;
- spark length rises as the pressure increases, amounting to 3-5 mm;
- at higher pressures the plasma loses its symmetry – its part faced to the laser dominates absorbing major part of the laser energy.

Absorption of the laser energy, $I_{abs}/I_0 = e^{-\mu x}$

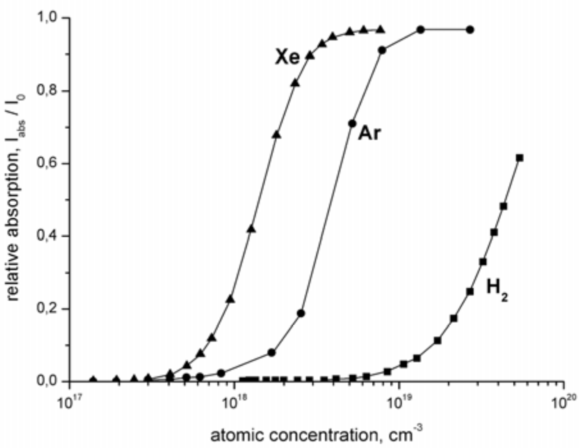

Xe – E_{las} = 0.60 J,

Ar – E_{las} = 0.63 J,

H_2 – E_{las} = 0.59 J

Absorption coefficient, μ

$$\mu = \frac{4\pi e^2}{m_e c}\frac{n_e \nu_{ei}}{\omega^2} = \frac{4\pi e^2}{m_e c}\frac{n_e n_i \langle \sigma_{ei} V_e \rangle}{\omega^2} = \frac{16\pi^2 e^6}{(3m_e)^{3/2} c} L_C \frac{Z^3 n_i^2}{\varpi^2 (k_B T_e)^{3/2}}$$

Values of μ can be easily deduced from the measured absorption, I_{abs}/I_0 , and the plasma temperature, Te, could be derived if the average ion charge, Z, were known.

<u>Hydrogen plasma</u> temperature (Z = 1)

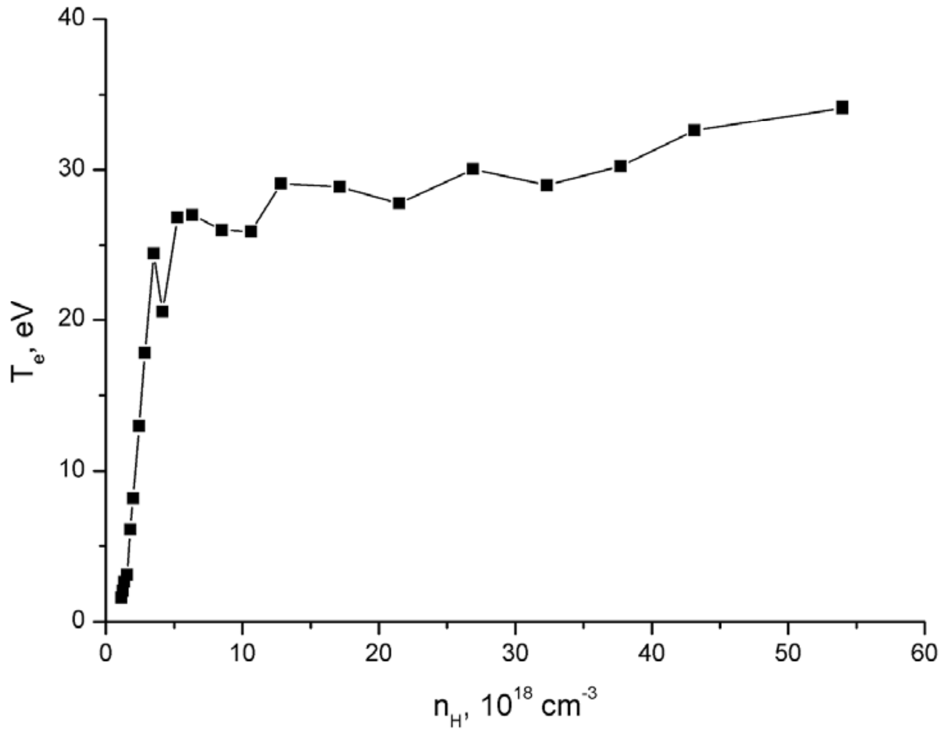

- **<u>In Xe laser plasmas</u>, if Z = 9 to 11, $T \approx$ 30 eV too.**
- **<u>In Ar laser plasmas</u>, if $T \approx$ 30 eV, the ion charge Z = 5-6.**
- **<u>Is the laser plasma a sort of "thermostatic system"?</u>**

Evolution of the laser plasma in time.

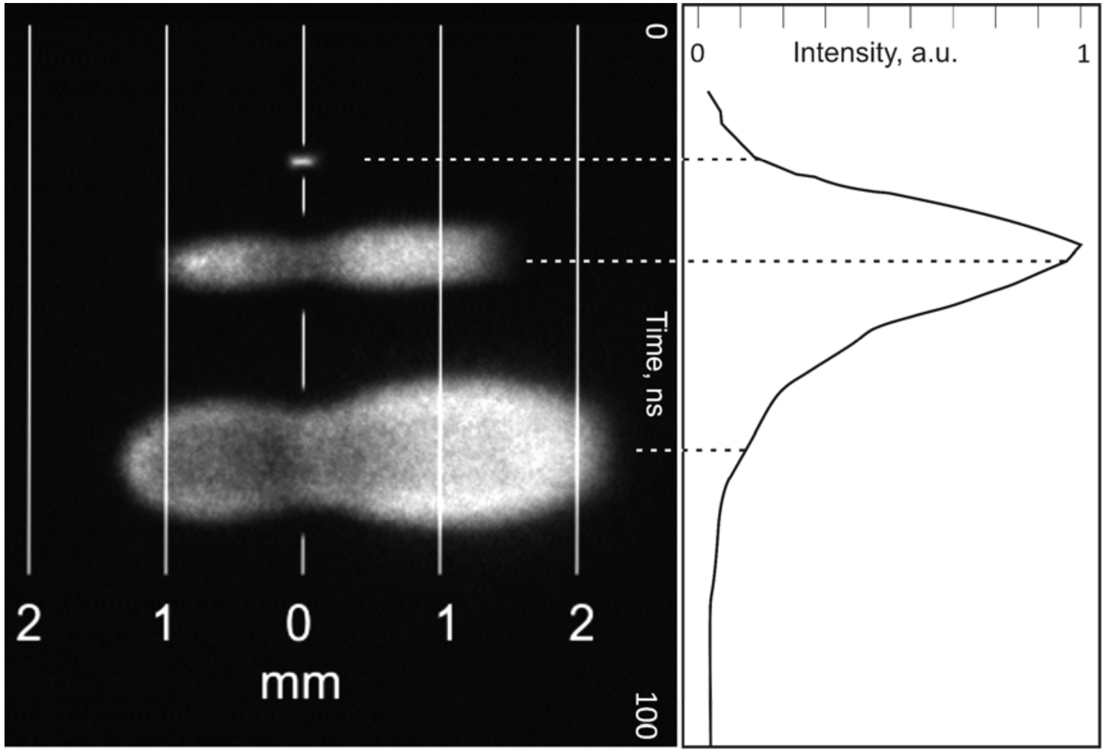

Snap-shots of the plasma spark in Ar.

P = 162 Torr, E_{las} = 535 mJ, I_{abs}/I = 75%.

BIFO K008 streak&uniframe camera was used. Exposition – 1.8 ns.

The laser is on the right of the spark.

Shot moments are shown in relation to the laser pulse waveform.

Distances of the light front from the focus vs. time

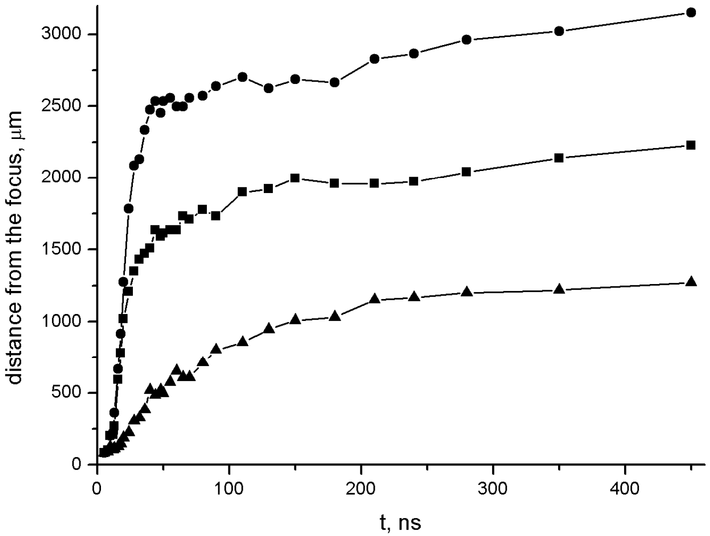

Plasma boundary motion in different directions from the focus:

—●— – toward the laser;

—■— – backward from the laser;

—▲— – across the beam in focal plane.

- Velocities from 10^6 down to 10^5 cm/s can be explained with shock waves, but those close to 10^7 cm/s can not.
- Primary electrons born by the multiphoton ionization are cold (about 1 eV) and unable to excite/ionize atoms.
- They gain the energy from the electromagnetic wave through collisions with atoms but intensity of the laser radiation goes down with the distance from the focus, *L*.

Time of accumulation of the energy necessary for the ionization

$$\tau_i = \frac{E_i (kL)^2 m_e c \omega^2}{4e^2 W_{las}} \times \frac{1}{n_a \sigma_{ea} < V_e >}$$

Below is time of the plasma light appearance in a point on the beam axis vs. its distance from the focus:

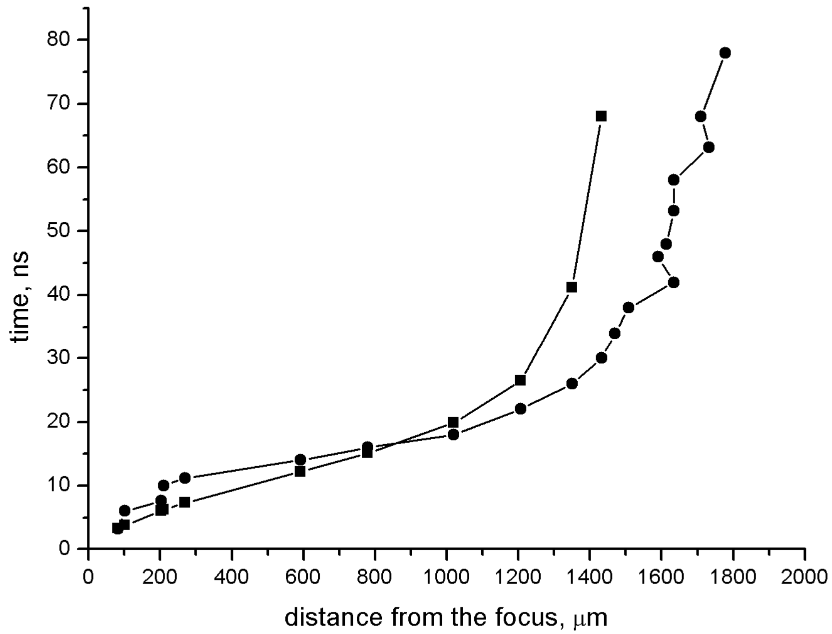

–●– – experiment (inverted curve from the previous figure)

–■– – calculation

Some peculiarities more – "protuberances and satellites“ observed in Xe within a narrow pressure range

Xe, P = 9 Torr, t = 22 нс

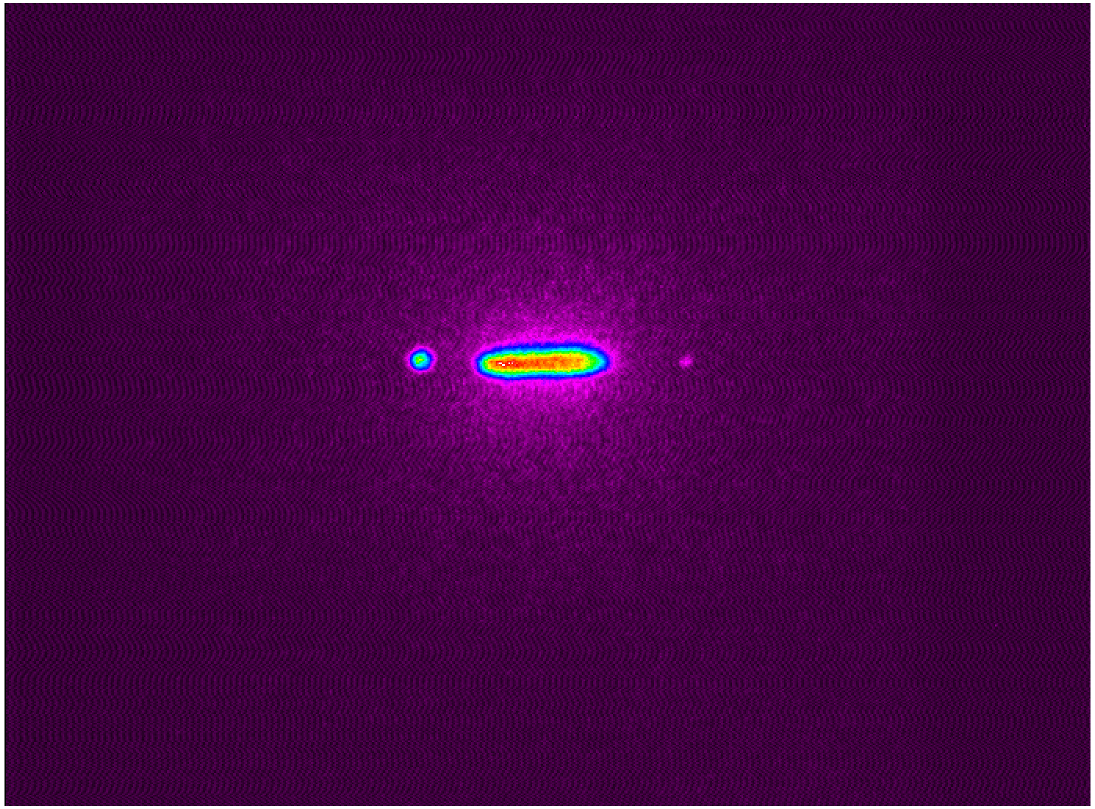

Computational optimization of the gas-jet target in the LPP short-wave radiation source (Poster session, P12)

Goal of this part of our work is search for optimum target jet configurations – with the highest possible core density to enhance the plasma emission and the least possible peripherical absorption.

1st phase – Fluid Mechanics Simulation (FMS) of the gas jet outflowing from a nozzle into the vacuum

Set of nozzles to be calculated:

No.	**1**	**2**	**3**	**4**	**5**	**6**	**7**
r_{cr} (mm)	0.1	0.2	0.1	0.1	0.1	0.1	0.1
r_{ex} (mm)	0.55	0.55	0.1	1.1	0.55	0.55	0.55
l (mm)	13	13	13	13	17	6	25

Primary data – fields of gas flow parameters for P_0 = 1÷10 atm and T_0 = 293 and 200 ºK

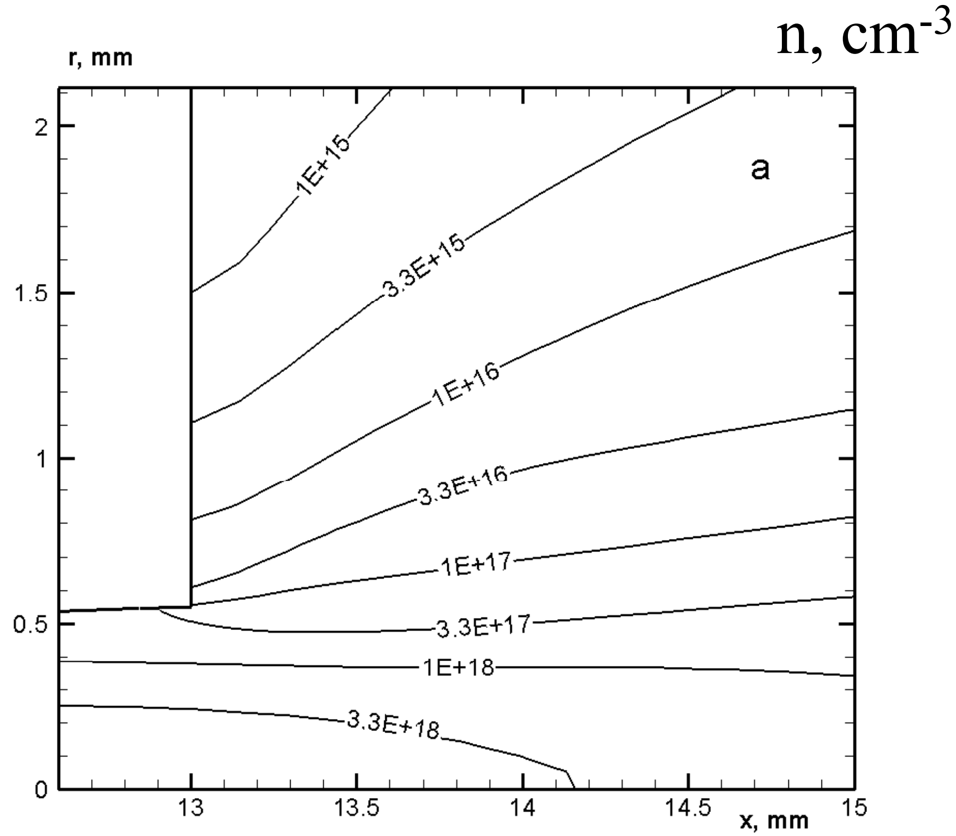

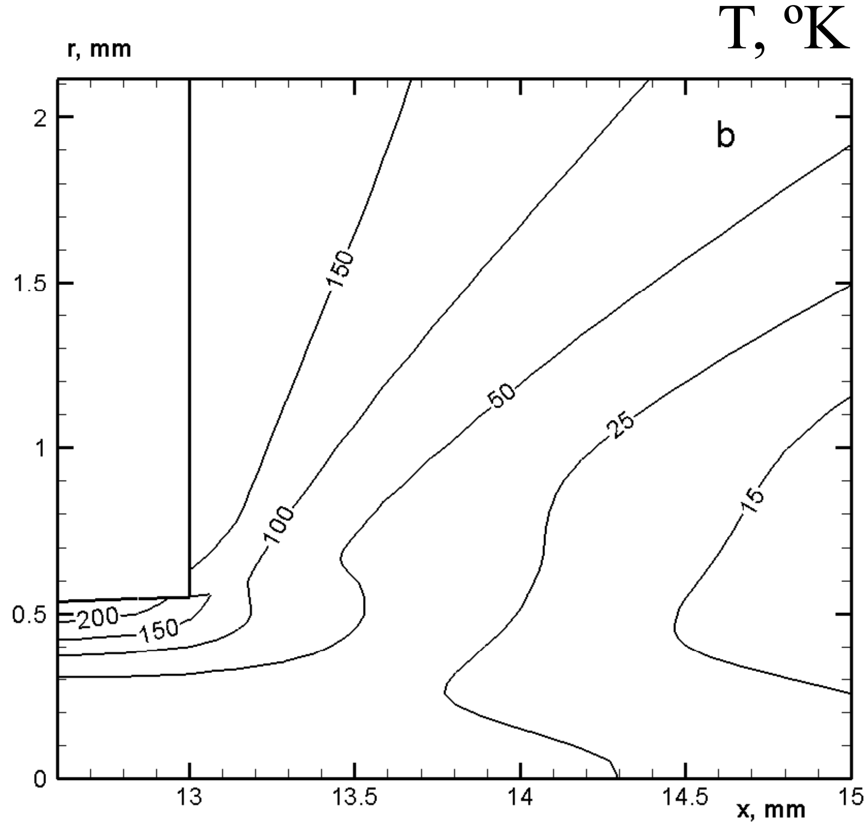

Radial profiles of Xe atomic concentration

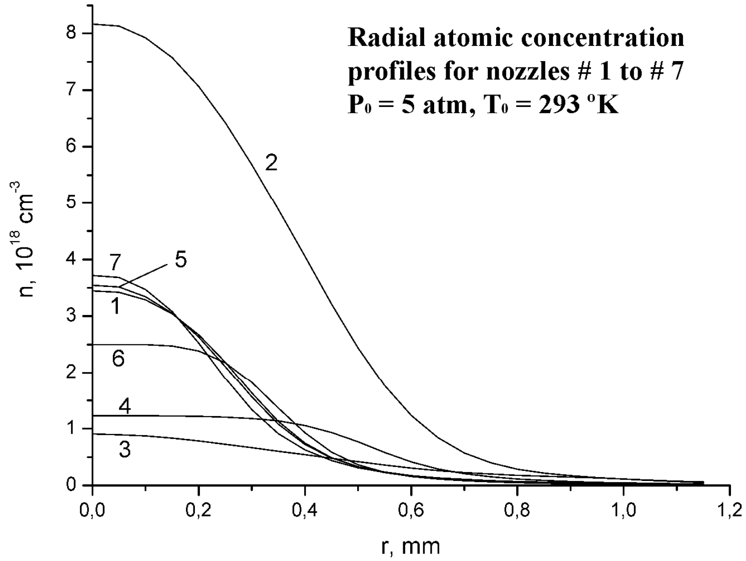

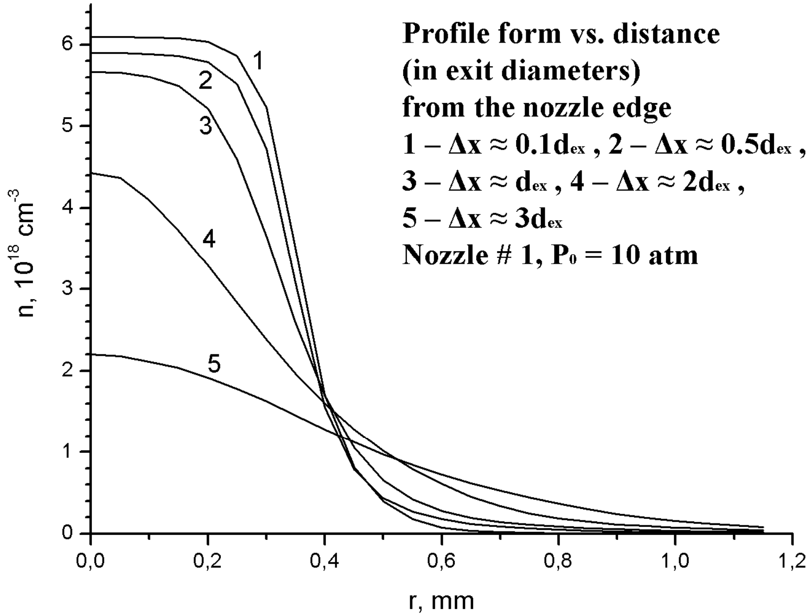

Huge number of profiles, variability of their forms provide no reasonable selection of the optimum.

<u>2nd phase</u> – combined optimization parameter

describing plasma emission as seen by an external observer

$$F = \langle n^2 l \rangle_{pl} \exp\{-\sigma_{abs} \langle nl \rangle_{peri}\}$$

$\langle n^2 l \rangle_{pl}$ – integral of n^2 over chord of observation inside the plasma describes the plasma emissivity;

$\langle nl \rangle_{peri}$ – integral of n over line of sight from external plasma boundary to the observer, so that exp{...} is absorption factor;

σ_{abs} = 2.365×10^{-17} cm^2 is maximum absorption cross-section for Xe

Application of the F-factor

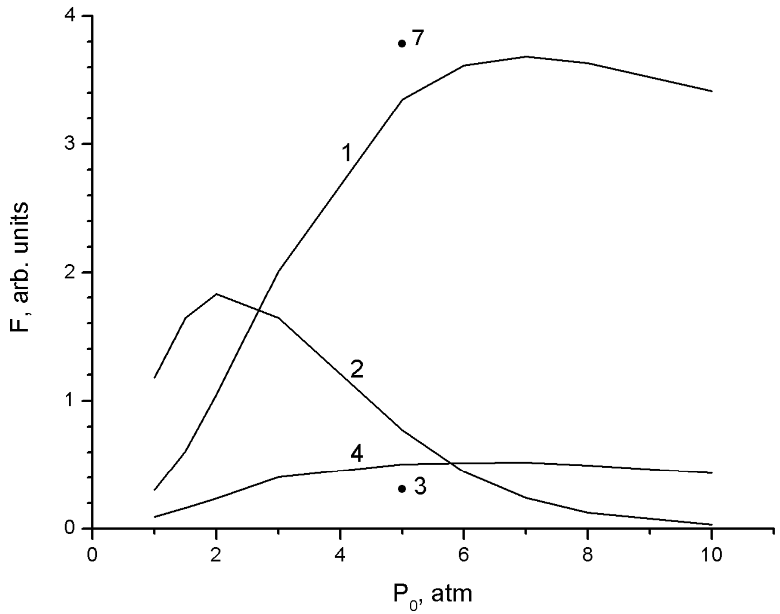

Application of the F-factor based on FMS data provides a reliable choice of optimum nozzle configuration, initial gas conditions, and location of the focus relative to the nozzle axis and edge.

Above: F-factor vs. initial pressure for different nozzles at central position of the focus.

Right: F-factor for different nozzles at different initial gas conditions vs. shift of the focus point from the jet to the observer.

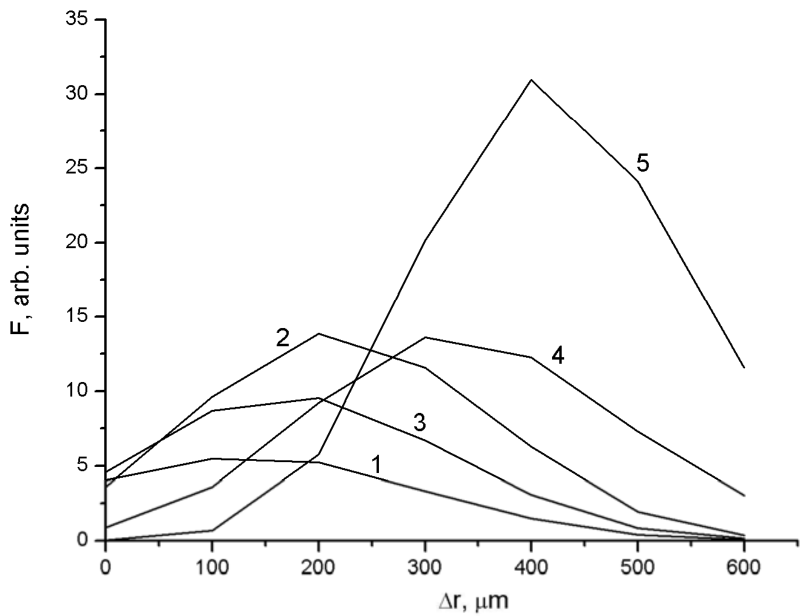

Publications in journals

- S. G. Kalmykov. Technical Physics Letters, Vol. 34 (2008), No. 9, p.p. 757-759.
- S. G. Kalmykov. Technical Physics Letters, Vol. 35 (2009), No. 11, p.p. 1020-1022.
- A. V. Garbaruk et al. Technical Physics Letters, Vol. 36 (2010), No. 12, p.p. 1072-1075.
- A. V. Garbaruk et al. Technical Physics, to be published in 2011.
- S. G. Kalmykov et al. Technical Physics Letters, to be published in 2011 (two articles).